Supporting Information for

STING activation promotes robust immune response and tumor regression in glioblastoma models

Gilles Berger,[1,2,3,*] Erik H. Knelson,[4] Jorge L. Jimenez-Macias,[1] Michal O. Nowicki,[1] Saemi Han,[4] Eleni Panagioti,[1] Patrick H. Lizotte,[4,5] Kwasi Adu-Berchie,[3] Alexander Stafford,[3] Nikolaos Dimitrakakis,[3] Lanlan Zhou,[6] E. Antonio Chiocca,[1] David J. Mooney,[3,7] David A. Barbie,[4] Sean E. Lawler[1,*]

[1] Harvey Cushing Neuro-Oncology Laboratories, Department of Neurosurgery, Brigham and Women's Hospital, Harvard Medical School, Boston, MA, USA.

[2] Microbiology, Bioorganic and Macromolecular Chemistry, Faculty of Pharmacy, Université Libre de Bruxelles, Brussels, Belgium.

[3] Wyss Institute for Biologically Inspired Engineering, Harvard University, Cambridge, MA, USA.

[4] Department of Medical Oncology, Dana-Farber Cancer Institute, Boston, MA, USA.

[5] Belfer Center for Applied Cancer Science, Boston, MA, USA.

[6] Legorreta Cancer Center at Brown University; Joint Program in Cancer Biology, Brown University and Lifespan Cancer institute; Department of Pathology and Laboratory Medicine, Warren Alpert Medical School, Brown University, Providence, RI, USA.

[7] Harvard John A. Paulson School of Engineering and Applied Sciences, Harvard University, Cambridge, MA, USA.

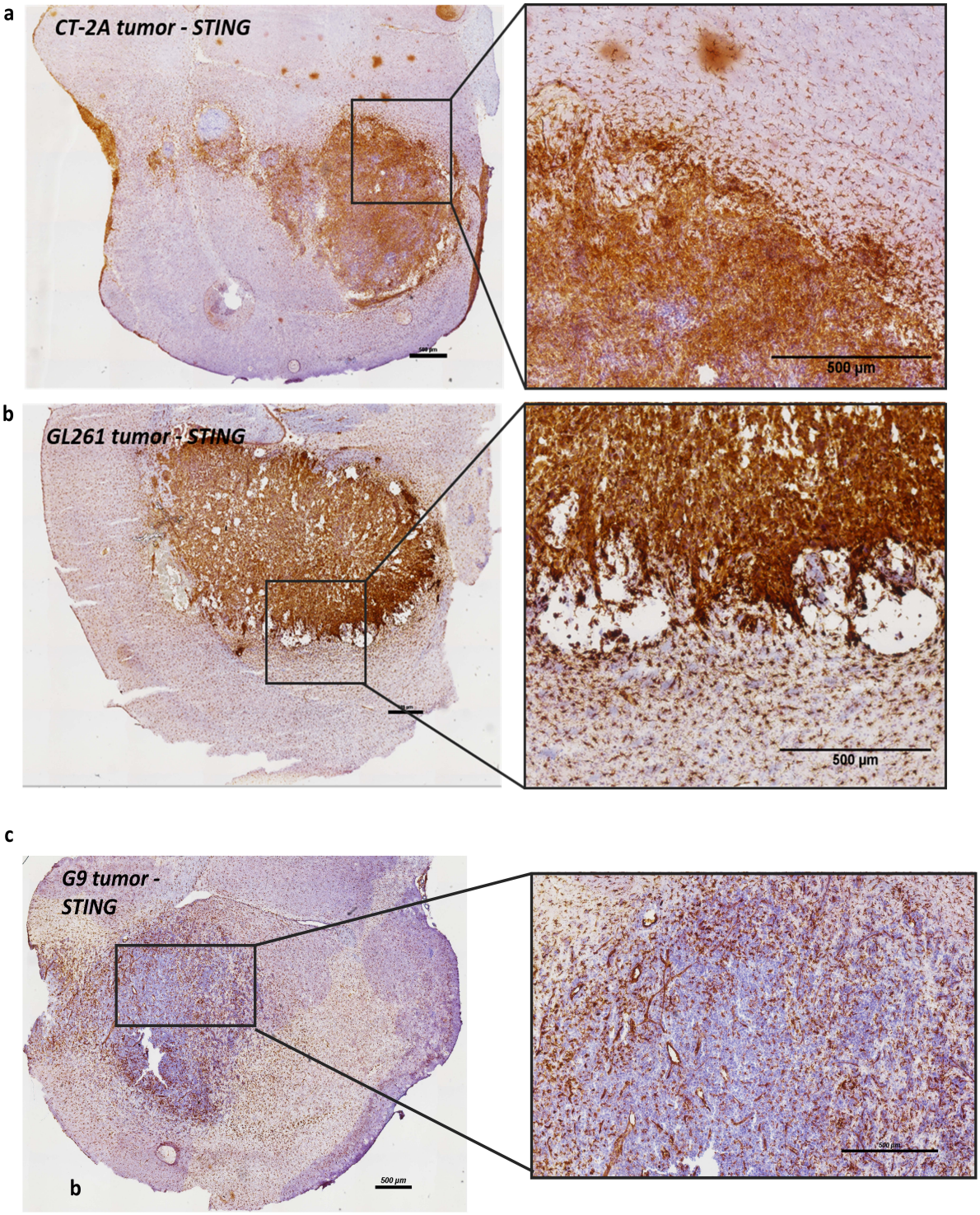

Figure S1. STING immunostaining on mouse tumor models. a, b, STING IHC staining of established murine CT-2A and GL261 tumors, showing STING is widely expressed in the tumor and expressed in a subset of cell in the healthy tissue. **c,** STING IHC staining for a G9 xenograft tumor; the bulk of the tumor does not express STING to visible levels.

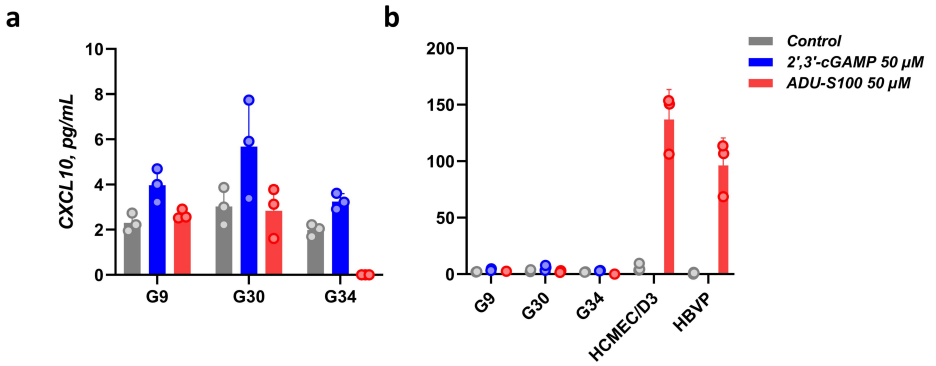

Figure S2. CXCL10 production following STING activation by 2',3'-cGAMP and ADU-S100. **a**, Levels of CXCL10 as measured by ELISA 24 h after STING agonist treatment of the indicated human GBM cell neurosphere lines. **b**, The same graph with the addition of responsive human brain endothelial HCMEC/D3 and brain pericyte HBVP cells to allow comparison.

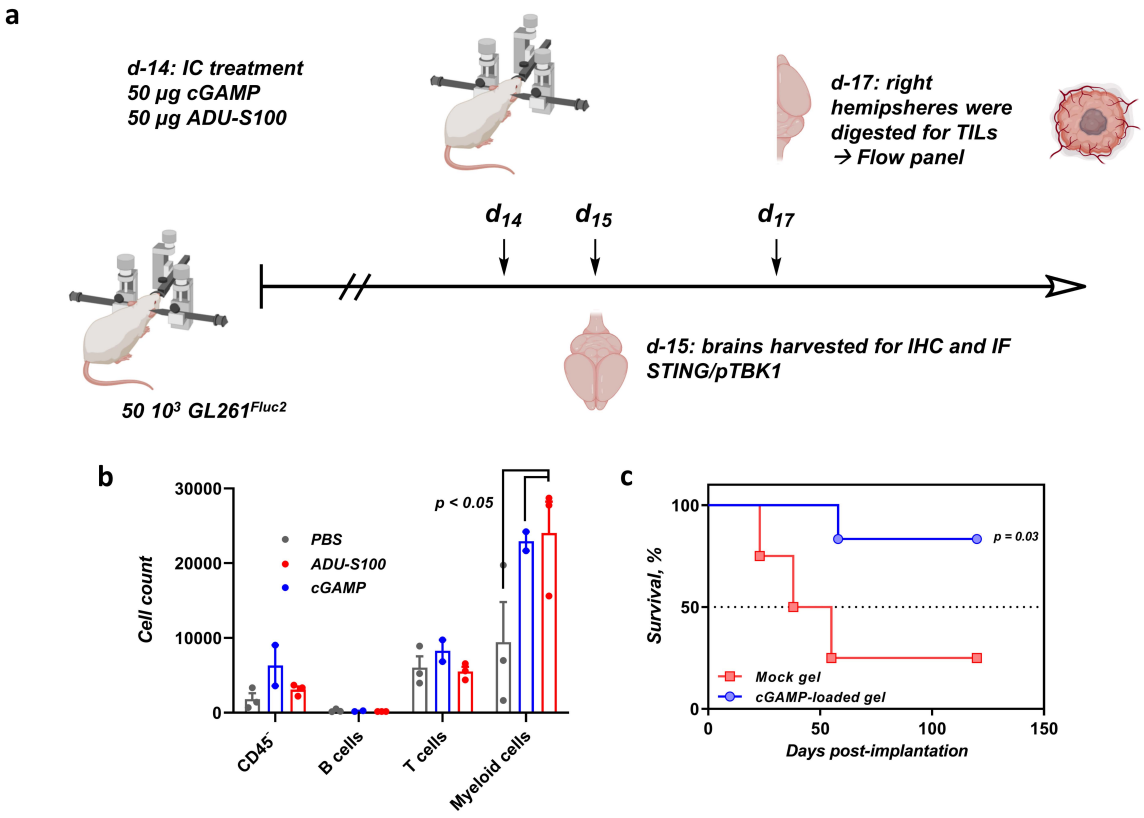

Figure S3. Pilot *in vivo* STING experiment. **a**, Timeline of the experiment. **b**, Flow cytometry analysis of the BILs 3 days after treatment with a bolus of either cGAMP or ADU-S100 in PBS (50 µg). **c**, Kaplan-Meier survival analysis from a cohort implanted with cGAMP-loaded hydrogels (100 µg).

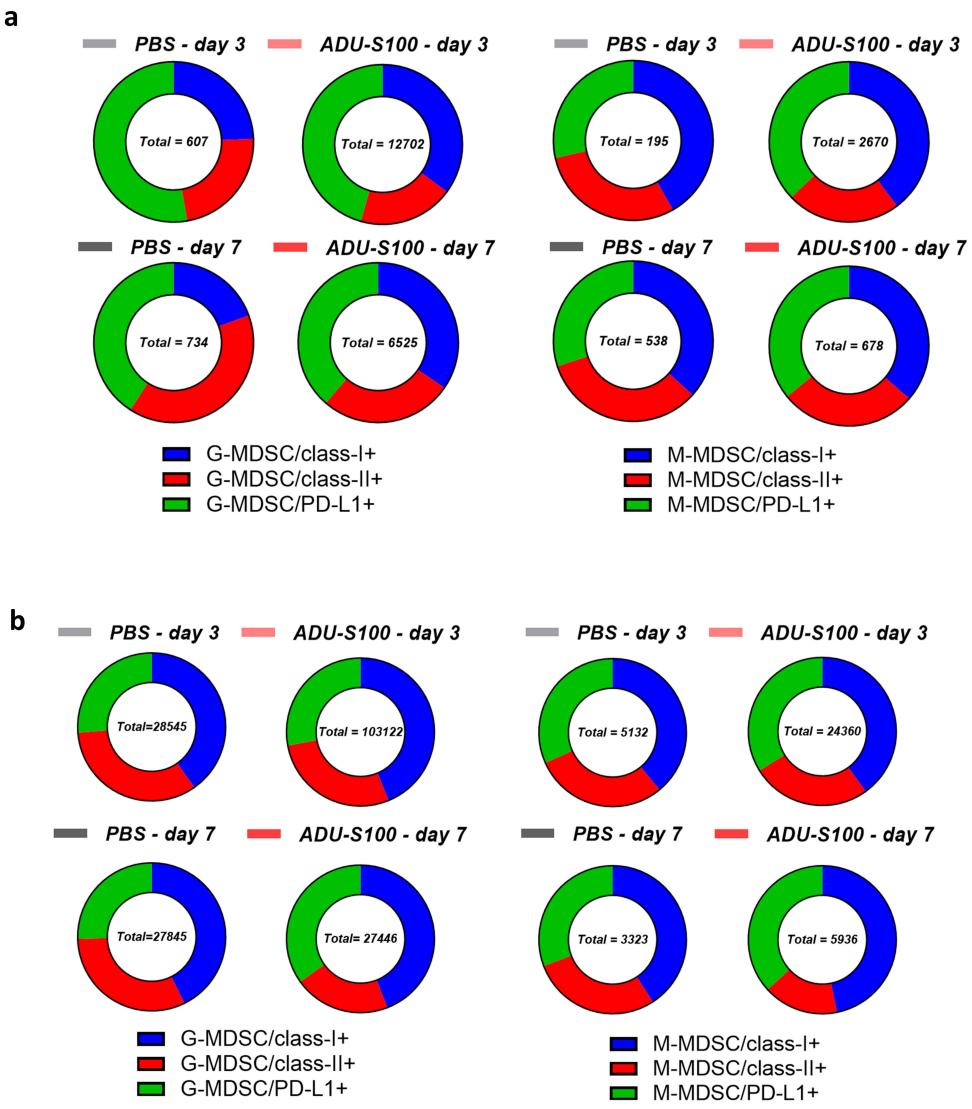

Figure S4. Flow cytometry analysis of brain MDSC populations following STING activation by ADU-S100. a, b, Expression levels of MHC class I/II and PD-L1 on G-MDSC and M-MDSC from BILs extracted from GL261 and CT-2A established tumors in controls and ADU-S100 treated conditions (respectively a and b).

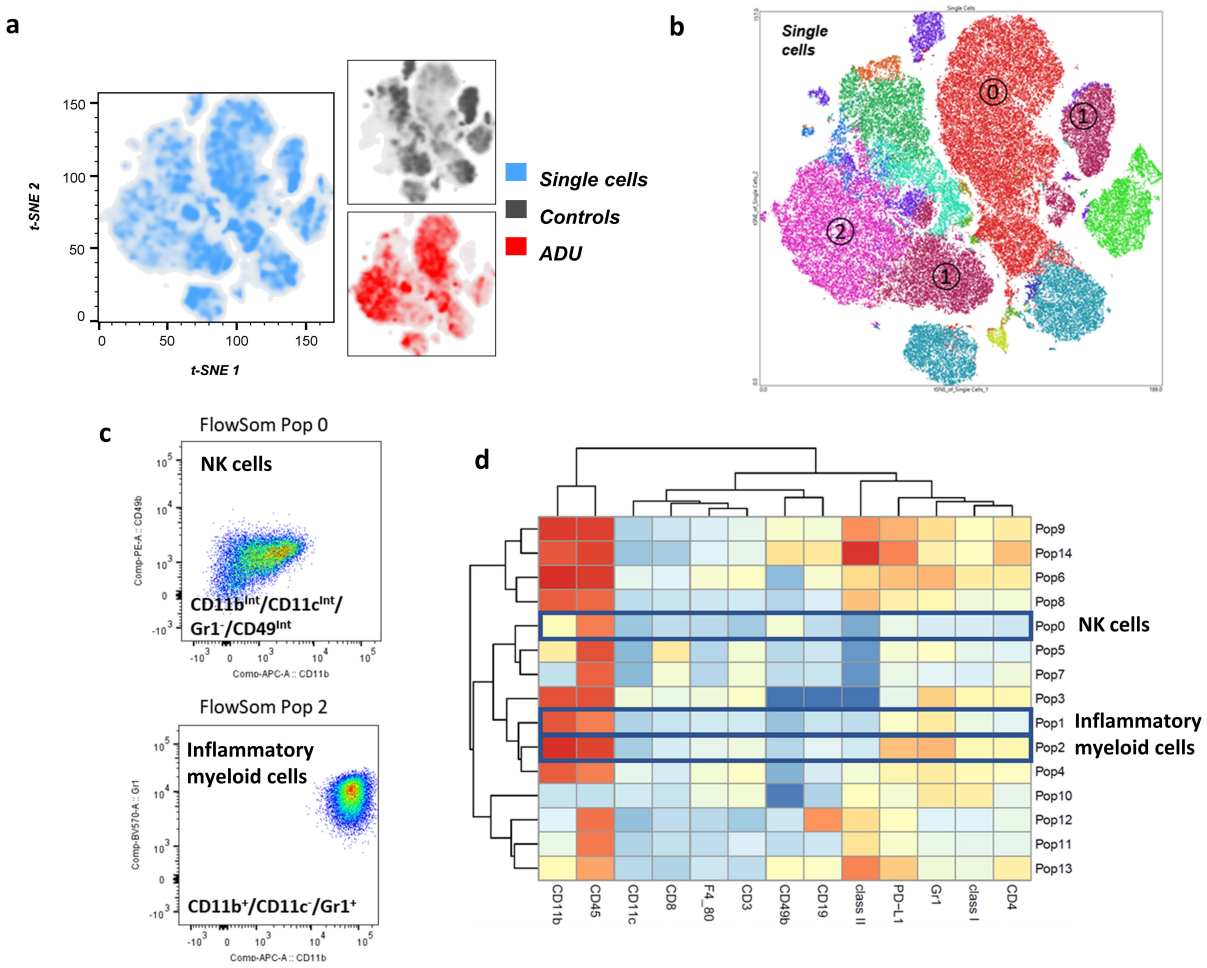

Figure S5. Assessment of CT-2A tumor immune infiltrates: figures at day 7 after STING agonist treatment. **a**, 2D t-SNE plots at day 7 post-treatment of established CT-2A tumors with ADU-S100 treated mice (50 µg, bolus) in red and controls in dark grey. **f**, t-SNE map for treated mice at day 7 colored by the FlowSOM populations; with relevant cell types highlighted. **c**, highly upregulated populations, comprising NK and inflammatory cells. **d,** Heatmap and hierarchical clustering of the FlowSOM populations at day 7.

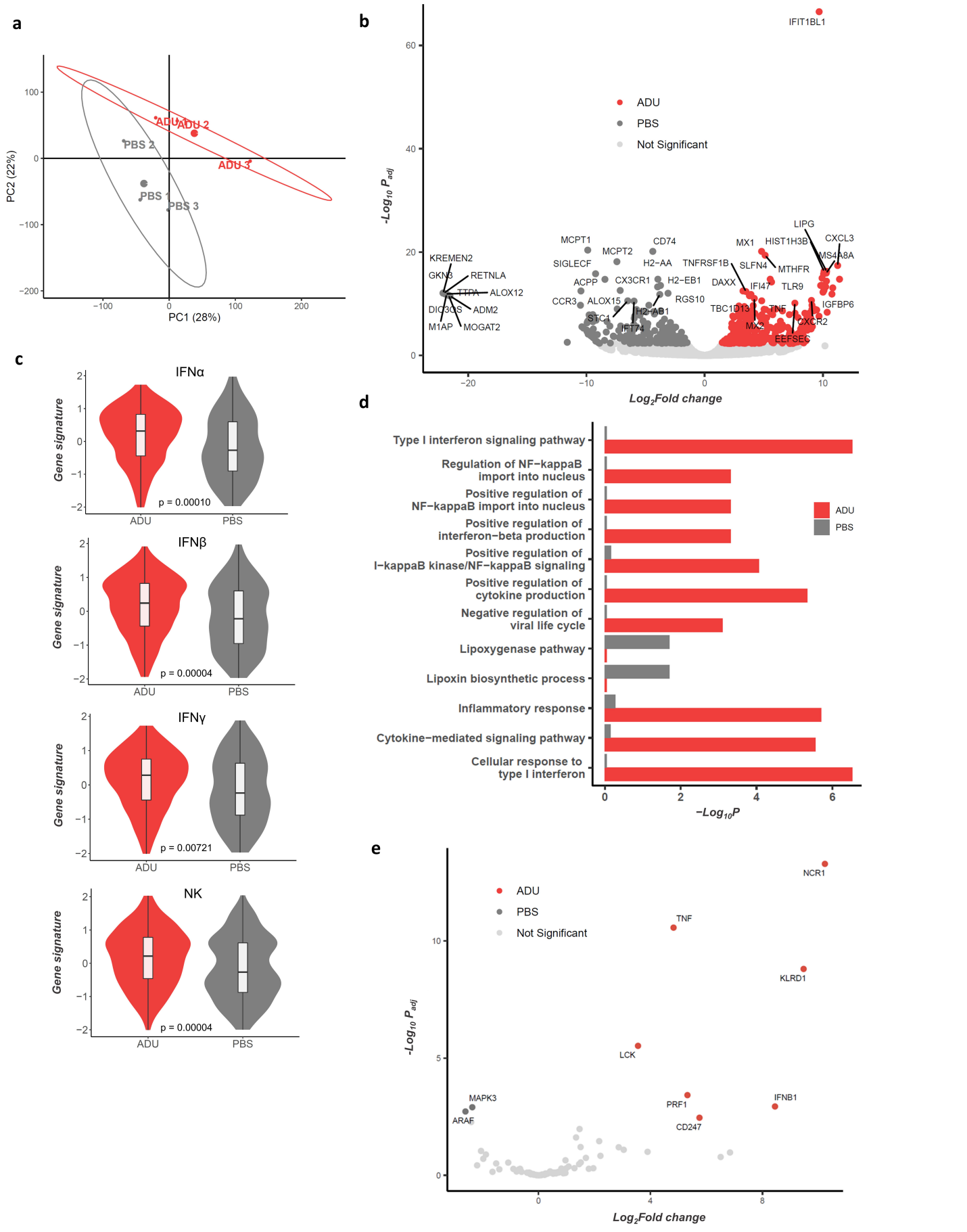
a
PC2 (22%)
PC1 (28%)
ADU 1
ADU 2
ADU 3
PBS 1
PBS 2
PBS 3
b
-Log10 Padj
Log2Fold change
ADU
PBS
Not Significant
IFIT1BL1
KREMEN2
GKN3
RETNLA
TTPA
ALOX12
DIO3OS
ADM2
M1AP
MOGAT2
MCPT1
MCPT2
CD74
SIGLECF
H2-AA
ACPP
CX3CR1
H2-EB1
CCR3
ALOX15
RGS10
H2-AB1
STC1
IFIT3
MX1
HIST1H3B
CXCL3
LIPG
MS4A8A
TNFRSF1B
SLFN4
MTHFR
DAXX
IFI47
TLR9
TBC1D13
TNF
IGFBP6
MX2
CXCR2
EEFSEC
c
IFNα
IFNβ
IFNγ
NK
Gene signature
p = 0.00010
p = 0.00004
p = 0.00721
p = 0.00004
ADU
PBS
d
Type I interferon signaling pathway
Regulation of NF−kappaB import into nucleus
Positive regulation of NF−kappaB import into nucleus
Positive regulation of interferon−beta production
Positive regulation of I−kappaB kinase/NF−kappaB signaling
Positive regulation of cytokine production
Negative regulation of viral life cycle
Lipoxygenase pathway
Lipoxin biosynthetic process
Inflammatory response
Cytokine−mediated signaling pathway
Cellular response to type I interferon
−Log10P
ADU
PBS
e
-Log10 Padj
Log2Fold change
ADU
PBS
Not Significant
NCR1
TNF
KLRD1
LCK
MAPK3
ARAF
PRF1
CD247
IFNB1

Figure S6. Transcriptome analysis from GL261 tumors treated with ADU-S100. a, PCA plot for individual samples, ellipsoids drawn with their centroids at the 95% confidence interval. The first two PCs are shown with their proportion of variance explained. Biologically independent animals per group, n = 3. **b**, Volcano plots for RNA sequencing data from GL261 BILs, ADU-S100 vs PBS showing differentially expressed genes (FDR adjusted *p* threshold ≤ 0.1.) **c**, Violin plots showing aggregate expression of IFN and NK-mediated cytotoxicity genes after ADU-S100 treatment of GL261 tumors. FDR adjusted *P* values (Wilcoxon) are given for each gene set (ADU-S100 vs PBS). **d**, Gene ontology analysis after ADU-S100 treatment of GL261 tumors. **e,** Volcano plot for RNA sequencing data from GL261 BILs, ADU-S100 vs PBS showing differentially expressed genes for the NK mediated cytotoxicity KEGG gene set. (FDR adjusted *p* threshold ≤ 0.1.).

Reference:

https://www.gsea-msigdb.org/gsea/msigdb/cards/KEGG_NATURAL_KILLER_CELL_MEDIATED_CYTOTOXICITY

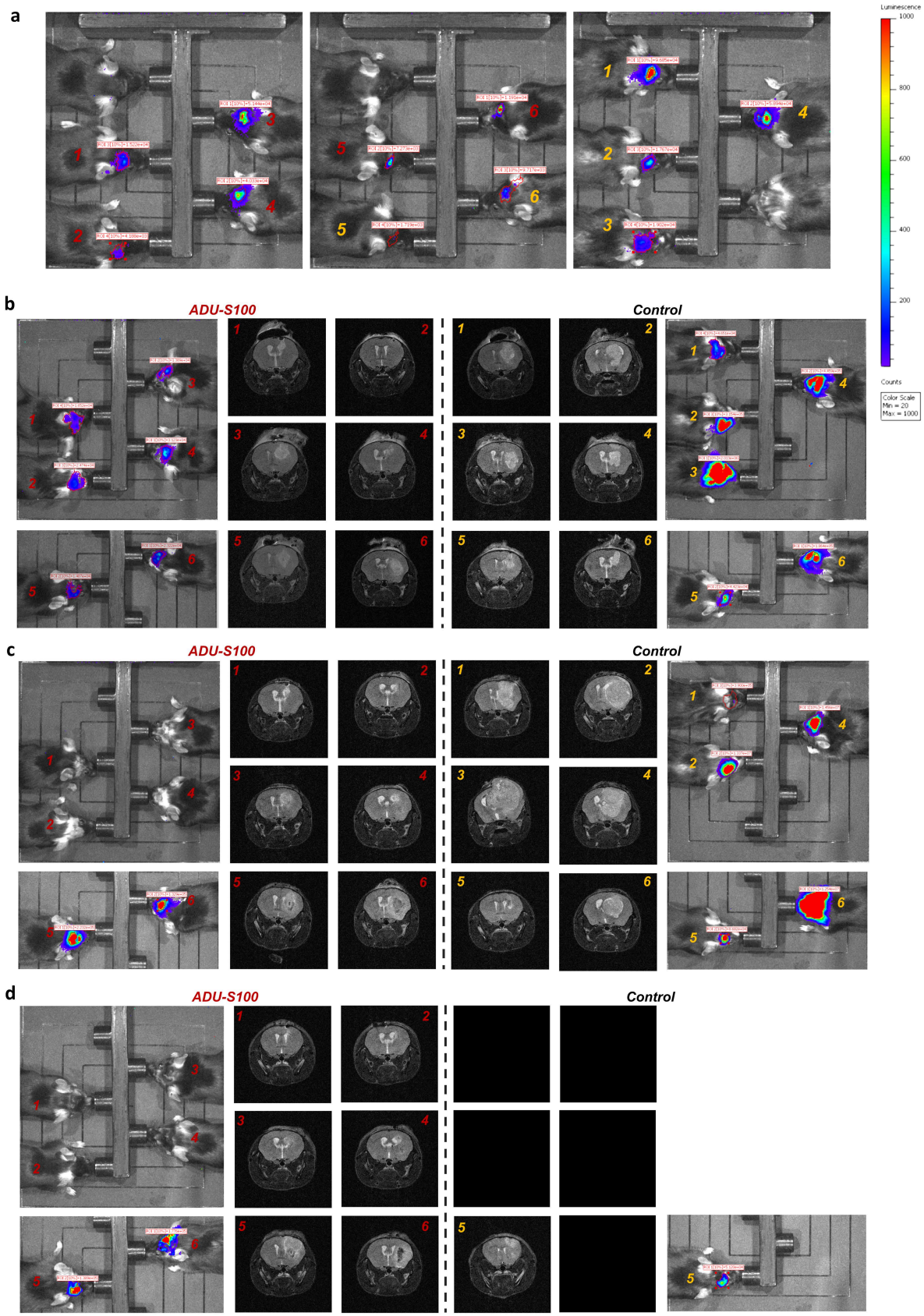

Figure S7. Therapeutic STING implants: GL261 survival. a, IVIS picture of both groups on treatment day. Mice without a clear IVIS signal are discarded from the study. **b, c and d,** IVIS and MRI of both groups at different timepoints.

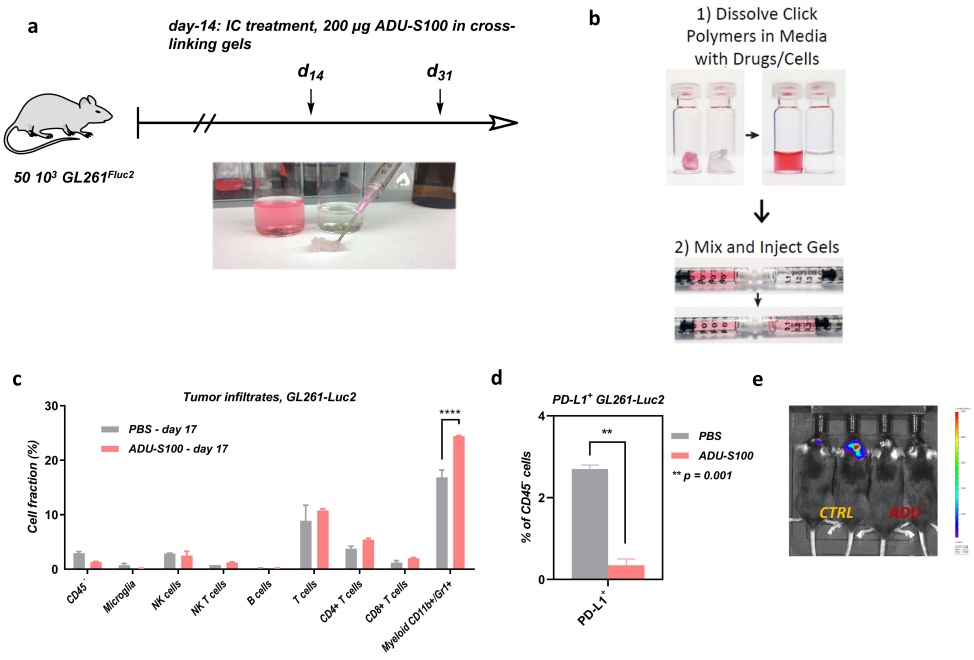

- ***PD-L1 no longer upregulated***
- ***Sustained increase in the macrophage population CD11⁺/Gr1⁺***

Figure S8. Long-term effect of therapeutic STING implants on the GL261 model. a, Timeline of the experiment. **b,** Graphical summary of the gel preparation. c, BIL flow panel 17 days after therapeutic gel implantation. **d,** PD-L1 expression on CD45$^-$ cells at the same timepoint. **e,** IVIS of the mice before sacrifice.

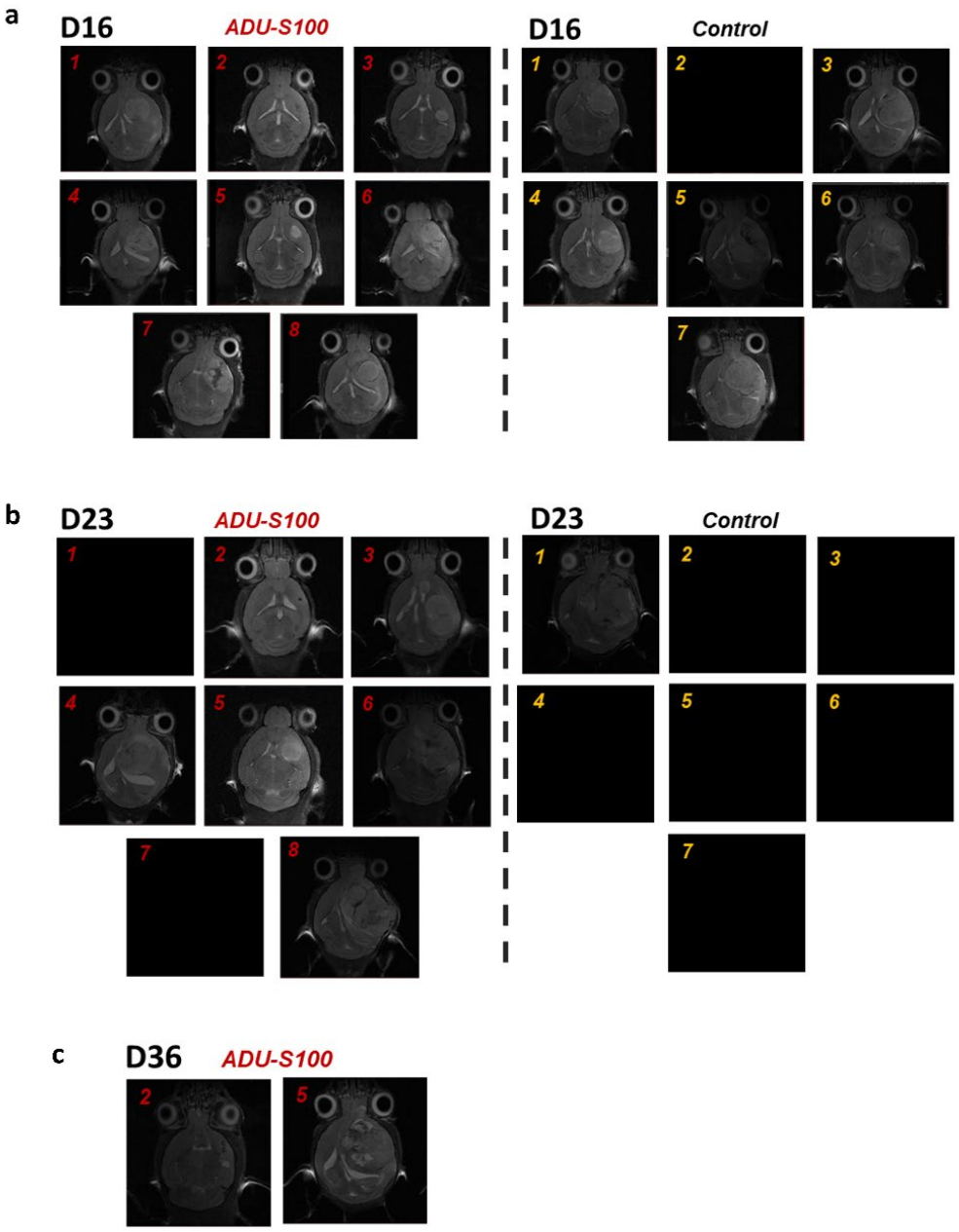

Figure S9. Therapeutic STING implants: CT-2A survival. a, b and c, IVIS and MRI imaging of both groups at different timepoints as shown.

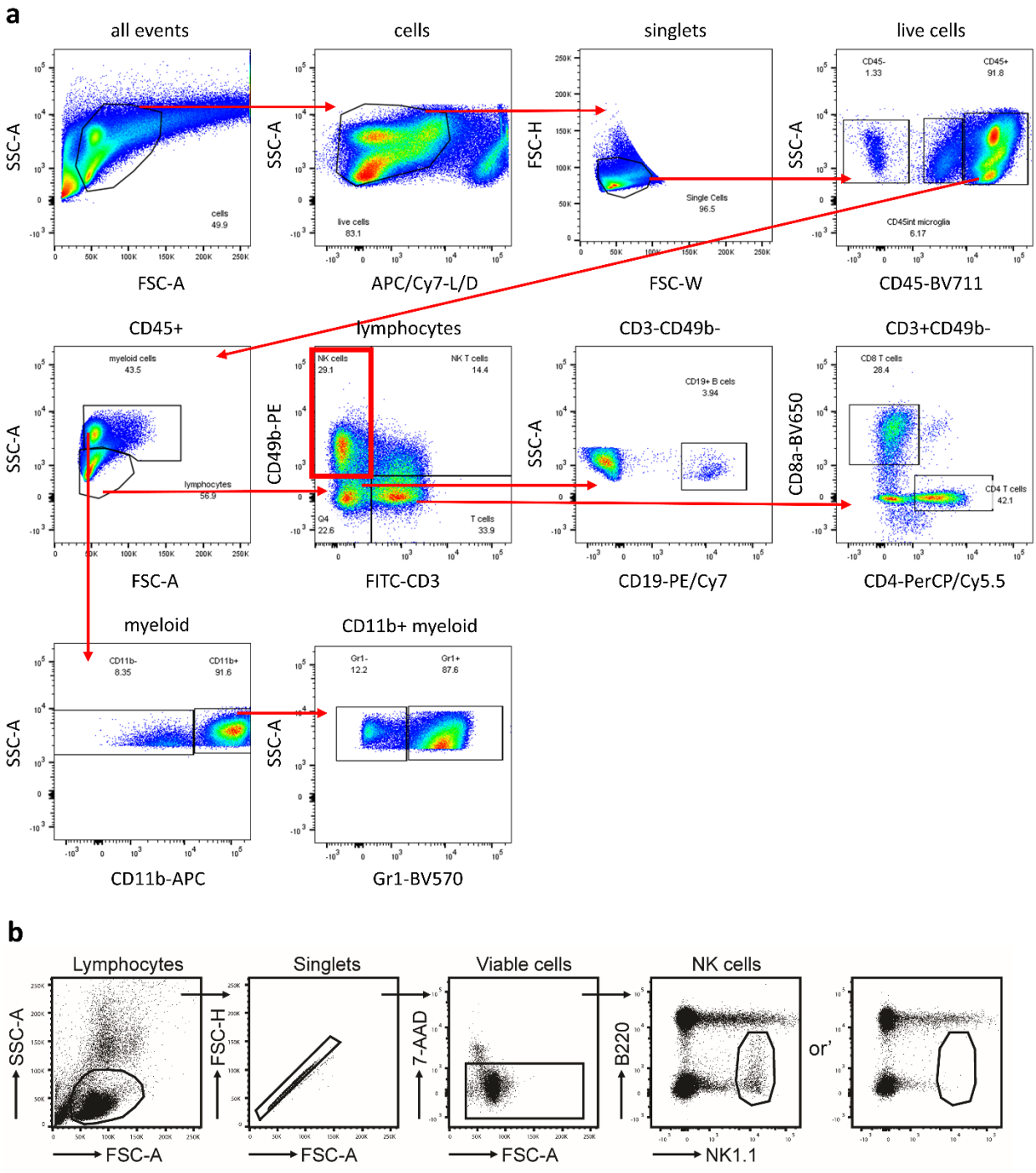

Figure S10. a, Gating strategies employed for the analysis of the TME and **b**, for the quantification of NK cells in peripheral blood.

Table 1. Mouse Flow Panel (all antibodies purchased from Biolegend, San Diego, CA).

CD3 FITC 100306	F4/80 BV421 123132
CD4 PerCP/Cy5 100434	H2KB BV510 116523
CD19 PE/Cy7 115520	GR-1 BV570 108431
CD49b PE 108908	CD8a BV650 100742
PD-L1 PE Dazzle 594 124323	CD45 BV711 103147
CD11b APC 101212	CD11c BV785 117335
MHC II AF700 107622	